A Fast-Response A-Film-Enhanced Fringe Field Switching LCD

Haiwei Chen,[1] Zhenyue Luo,[1] Daming Xu,[1] Fenglin Peng,[1] Shin-Tson Wu,[1]
Ming-Chun Li,[2] Seok-Lyul Lee,[2] and Wen-Ching Tsai[2]

[1]College of Optics and Photonics, University of Central Florida, Orlando, Florida 32816, USA
[2]AU Optronics Corp., Hsinchu Science Park, Hsinchu 300, Taiwan

Abstract

We proposed a new A-film-enhanced fringe field switching (A-FFS) LCD whose required dΔn value is only 50% of the conventional FFS. Fast response time can be achieved by decreasing the cell gap, while keeping transmittance over 90%. The parameters which may degrade the contrast ratio are addressed.

Keywords

Fringe field switching (FFS); Liquid crystal displays (LCDs).

1. Introduction

Fringe field switching (FFS) LCD has been widely used in mobile displays because of its outstanding features like high transmittance, wide view, weak color shift, and pressure resistance for touch panels [1, 2]. However, its response time still remains a challenge. To overcome this problem, reducing the cell gap is an effective approach [3]. Nevertheless, LC cell cannot provide enough phase retardation if cell gap is too thin, so the maximum transmittance is reduced.

In this paper, we propose a new FFS structure with an in-cell phase retarder, called A-FFS mode. A-FFS can maintain high transmittance with a thin cell gap. As a result, the response time can be improved without sacrificing the transmittance. With a carefully chosen A-film, good dark state can be achieved in the whole visible region.

2. Results

2.1 Device structure of A-film-enhanced fringe field switching (A-FFS)

Figure 1(a) shows the device configuration of conventional FFS structure. For dark state, the input linearly polarized light experiences no phase retardation after passing through the FFS cell, and is blocked by the crossed linear analyzer. In the fully on state, the FFS cell can be treated as a half-wave plate, through which the polarization of the outgoing light is rotated by 90°, so that it passes through the analyzer. It is obvious that there is a limit for conventional FFS, which is $d{\cdot}\Delta n$ must be larger than $\lambda/2$, otherwise the transmittance will decrease dramatically because the phase retardation is insufficient.

Here we propose a new device configuration depicted in Fig. 1(b), which only requires $d{\cdot}\Delta n \sim\lambda/4$. The key part of this new design is an A-film, which has the same phase retardation as the FFS cell ($d_A\Delta n_A{=}d_{LC}\Delta n_{LC}$), sandwiched between the polarizer and FFS cell. The working principle is the combination of A-film and FFS cell as a new phase plate. For convenience, we abbreviate this positive A-film-enhanced FFS cell as A-FFS.

When the axis of A-film is perpendicular to the FFS cell (here we use +A-film), the total phase retardation is zero (subtractive), leading to a good dark state. As the LC directors are reoriented by the electric field, phase retardation increases. When the additive phase equals to $\lambda/2$, a high transmittance bright state is obtained. Therefore, the new limit of A-FFS is $d_A{\cdot}\Delta n_A = d_{LC}{\cdot}\Delta n_{LC} = \lambda/4$, since $d_A{\cdot}\Delta n_A - d_{LC}{\cdot}\Delta n_{LC} = 0$, and $d_A{\cdot}\Delta n_A + d_{LC}{\cdot}\Delta n_{LC} = \lambda/2$.

The new A-FFS mode makes two important impacts: 1) If we keep d constant (same cell gap), then its Δn can be much smaller than the conventional one. Usually, the Δn of liquid crystal used in FFS cell is 0.09~0.12, but the Δn of A-FFS can be as low as 0.06, which is only one half of the original one. It means more freedom for us to choose the appropriate material used in FFS cell to get faster response time (lower viscosity) [4], since Δn is not a barrier any more. 2) If the Δn is kept the same, then the cell gap can be reduced, which in turn leads to faster response time.

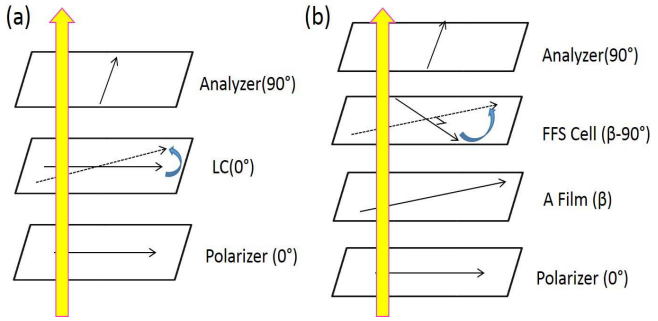

Fig. 1. Device structures of (a) conventional FFS and (b) A-FFS LCDs.

2.2 Polarization angle effect (β)

FFS cell is not a perfect phase plate because of the non-uniform LC reorientation induced by the electric field. In the on-state, n-FFS cell can be regarded as a double twisted nematic (TN) mode [4]. Thus we cannot determine the optimal angle between the polarizer and A-film intuitively. Here, we define it as polarization angle, labeled as β in Fig. 1(b).

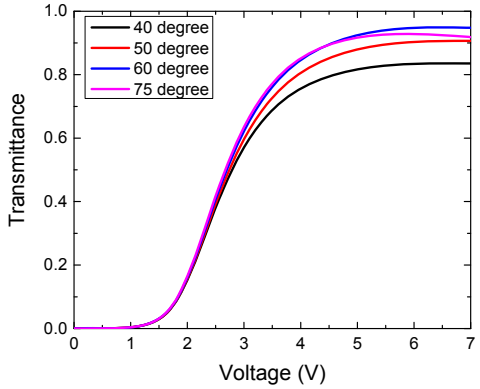

Fig. 2. Simulated VT curves of UCF-N1 at λ=550nm under different polarization angles.

 ISSN 0097-966X/15/4502-0656-$1.00 © 2015 SID

To investigate the polarization angle effect, a commercial LCD simulator DIMOS.2D is employed. In our simulation, we used UCF-N1 (Δn~0.119 at 550nm) and cell gap d= 3.02μm. The electrode width is 2μm, electrode gap is 3μm, and the rubbing angle is 10°. Figure 2 shows the VT curve of different polarization angles, and the highest transmittance is achieved when β = 60°. As a result, we do further investigation based on this optimal polarization angle (β=60°).

2.3 High transmittance

For conventional FFS mode, even though the phase is large enough ($d\Delta n > \lambda/2$) the transmittance is quite sensitive to the $d\Delta n$ value as shown in Fig. 3. However, this is not the case for our new A-FFS mode. Because the phase is not determined by the FFS cell only, it is the combination effect of A-film and LC cell, in which the A-film can supply an additional phase retardation to boost the transmittance.

In our new A-FFS, we can still get high transmittance as long as all the LC directors are reoriented by 90°, i.e. the total phase change is equal to π. Therefore, A-FFS mode has high transmittance, which is insensitive to the cell gap. As Fig. 3 shows, the transmittance of A-FFS mode keeps over 90%, while the transmittance of conventional FFS drops rapidly as $d\Delta n$ decreases.

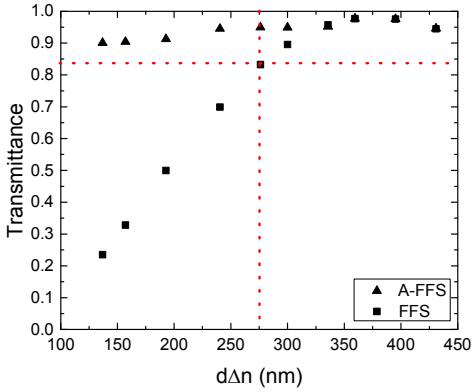

Fig. 3. Simulated transmittance of A-FFS at λ=550nm with different $d{\cdot}\Delta n$ values. (The intersection of two red dotted lines corresponds to $d{\cdot}\Delta n$=λ/2.)

2.4 Response time vs. cell gap

As cell gap decreases, response time decreases in proportion to d^2 [5]. Table 1 depicts this trend and lists the detailed data. From Table 1, both rise time and decay time get faster with the decreased cell gap. From the values listed in Table 1, we can get an appropriate quadratic relationship between response time and cell gap. When d=1.62μm, the total response time (rise time + decay time) is about 10 ms, which is 4x faster than that of conventional FFS mode.

Table 1. Simulated rise time and decay time of A-FFS at different cell gaps. λ=550 nm.

Cell Gap (μm)		3.02	2.82	2.52	2.32	2.02	1.62
Time (ms)	Rise	15.6	13.2	10	8	5.6	4.8
	Decay	23.2	19.2	16	13.2	10.4	6.4

For conventional FFS, the optimized $d\Delta n$ is about 0.65λ, which means the cell gap cannot be too thin. Otherwise, a large birefringence material is required, which could result in a higher viscosity. For FFS cell with d~2μm, the Δn should be as large as 0.18; but for A-FFS the required Δn~0.09. Thus, we can decrease the cell gap without worrying about Δn. It means the fast response time listed in Table 1 can be easily achieved by the present LC materials.

2.5 Cell gap tolerance

For A-FFS mode, $d_A\Delta n_A = d_{LC}\Delta n_{LC}$ should be satisfied in order to obtain a good dark state. However, the fabrication error has to be taken into consideration. To evaluate the $d\Delta n$ tolerance, we calculate the contrast ratio of different cell gaps while keeping the A-film thickness unchanged. Besides, we try to optimize the dark state by tuning the polarization angle (β), and the results are listed in Table 2. From Table 2, tolerance is the smallest when β=45°, and the tolerance range increases with increasing β. When β=80°, the tolerance range is ±4.5% with CR>2000, and ±8.6% with CR>400, which is acceptable for the industrial fabrication.

Table 2. Tolerance of $d\Delta n$ under different criteria with different β angles for $d_A\Delta n_A = d_{LC}\Delta n_{LC}$=λ/2. LC: UCF-N1 with d~2.32μm.

Contrast Ratio		>2000	>1000	>400
$d\Delta n$ tolerance	β=45°	±0.85%	±1.7%	±3.25%
	β=60°	±1.3%	±2.15%	±3.45%
	β=75°	±2.6%	±3.85%	±6.05%
	β=80°	±4.5%	±5.6%	±8.6%

2.6 Dispersion effect

It is fairly easy to design an A-film to satisfy $d_A{\cdot}\Delta n_A = d_{LC}{\cdot}\Delta n_{LC}$ at a given wavelength, say λ=550nm. However, the dispersion of both A-film and LC material could be mismatched at other wavelengths. For white light operation, the dark state of the proposed normally-black display will be degraded if there is mismatched dispersion. To solve this problem, we have to choose the A-film and LC material carefully so that their dispersion is the same. Fortunately, this problem has been addressed 20 years ago when dealing with the film compensation to widen the viewing angle [6].

The wavelength-dependent birefringence of liquid crystal could be described by [7]:

$$\Delta n(\lambda) = G\frac{\lambda^2 \cdot \lambda^{*2}}{\lambda^2 - \lambda^{*2}}, \quad (1)$$

where G is a proportionality constant and λ^* is the mean electronic transition wavelength. For Mylar and UCF-N1, λ^* is 224nm [8] and 219nm [9], respectively. Figure 4 depicts the wavelength dependent Δn of these two materials. The Δn shown in Fig. 4 is normalized to the Δn value at λ=550nm to avoid the scale difference. Excellent match is achieved in the visible region. Thus with Mylar as the A-film material, the contrast ratios for red (650nm), green (550nm) and blue (450nm) are found to be 1784, 2914 and 1472, respectively, which is pretty good for mobile displays.

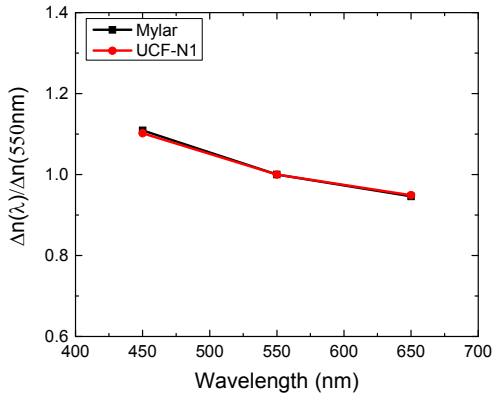

Figure 4. Wavelength dependent Δn of UCF-N1, Mylar film, and polycarbonate film.

2.7 The position of A-film

All the results above are obtained with A-film sandwiched between the polarizer and the LC cell, which means the input linearly polarized light passing through A-film first. Next, we investigate the order effect by exchanging the positions of A-film and LC cell, as illustrated in Fig. 5(a) and (b). Theoretically speaking, the results should be the same whether the light comes from the polarizer side (upward) or from the analyzer side (downward). Fig. 5(c) shows this effect, from which we can see the transmittance for both cases is the same except for a shifted phase (~90˚).

2.8 Positive A-FFS

The proposed A–FFS mode not only offers superior performances with negative $\Delta\varepsilon$ LC materials, but it also works well with positive LCs. Fig. 6(a) and 6(b) show the simulated transmittance and polarization effect using a positive $\Delta\varepsilon$ LC material (MLC-6686, Δn~0.0983 at λ=550nm), respectively. Same as the negative A-FFS mode, the optimized polarization angle for the positive A-FFS is also 60˚. Nevertheless, the transmittance does not stay above 90% as the negative A-FFS shown in Fig. 3. For a positive $\Delta\varepsilon$ LC, its directors tend due to follow the electric field. In the middle of electrodes and gaps, the electric fields are largely in vertical direction. These vertically reoriented LCs do not contribute to transmittance. As a result, dead zones are formed and transmittance decreased. In spite of this shortcoming, A-FFS still exhibits a much higher transmittance than the corresponding FFS mode as Fig. 6(a) depicts.

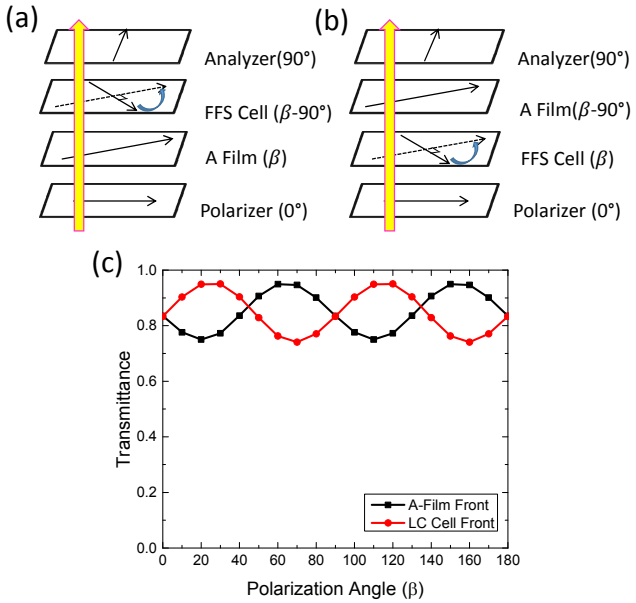

Fig. 5. Structures for both cases: (a) A-film front, (b) LC cell front, and (c) transmittance with different polarization angles.

3. Discussion

The theoretical $d\Delta n$ limit for conventional FFS is $\lambda/2$. However, the LC directors near the substrates are subject to strong surface anchoring so that they do not contribute to the phase retardation. In practical applications, we have to increase the $d\Delta n$ value to, say 0.65λ, in order to obtain high transmittance and low operation voltage [10]. Similarly for A-FFS, its $d\Delta n$ value should be larger than the theoretical limit, which is $\lambda/4$. During the above calculations, we set $d\Delta n=\lambda/2$. Obviously, this value can be further decreased to enable a thinner cell gap for faster response time, but the major trade-off is increased voltage. To lower operation voltage, several approaches can be used, e.g. reducing the passivation layer thickness, decreasing the rubbing angle, and increasing the dielectric anisotropy of the LC employed [11].

For smart phones and pads operated by battery, low voltage helps to reduce power consumption and lengthen battery's life. But for large-screen TVs or computer screens, a higher operation voltage (7.5V) can be tolerated because the major power consumption comes from the backlight [12]. Especially for TVs, fast response time plays a key role to suppress motion picture image blurs. Under such condition, the advantages of A-FFS clearly manifest because it allows a thinner cell gap to be used for achieving fast response time. To illustrate this feature, we compare the VT curves of A-FFS and FFS at $d\Delta n$=240nm, as Fig. 7 depicts. From Fig. 7, A-FFS reaches 95% transmittance at 7.5V, but the peak transmittance of FFS saturates at 70% although its voltage is only 6V.

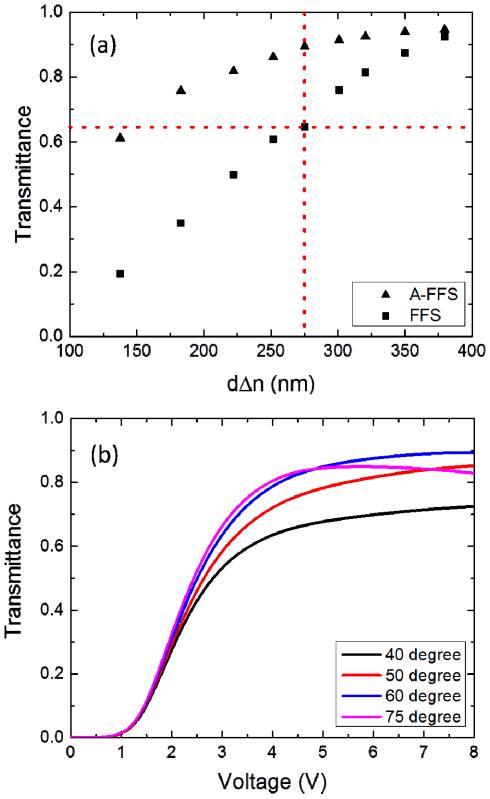

Fig. 6. Simulated results for A-FFS using a positive $\Delta\varepsilon$ LC (MLC-6686) at 550nm: (a) transmittance with different cell gaps, and (b) VT curves under different polarization angles.

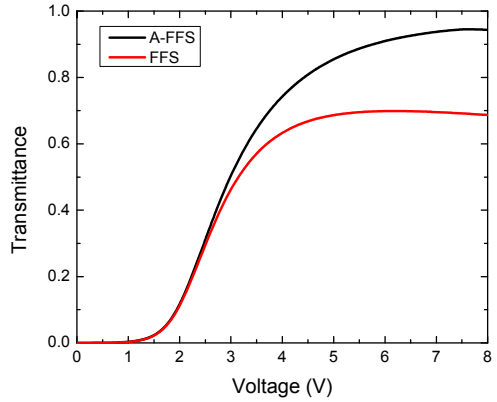

Figure 7. Simulated VT curves for A-FFS and FFS using UCF-N1 at λ=550 nm with $d\Delta n$=240nm.

For FFS mode, especially n-FFS ($\Delta\varepsilon$<0), the electric-field-induced molecular reorientation takes place primarily in the horizontal direction, which results in very wide viewing angle. Since the working mechanism of A-FFS is the same as conventional FFS (in-plane molecular reorientation), the wide view property will be persevered [13]. As shown in Fig. 8, A-FFS has a similar isocontrast performance with conventional FFS, and the contrast ratio (CR) remains over 100:1 in the entire viewing zone (±80°). What's more, with the emerging quantum dot (QD) enhanced backlight, the colour performance (e.g. colour shift and colour gamut) will be greatly improved. And superior image quality at outdoor environment and high optical efficiency could also be achieved [14-15].

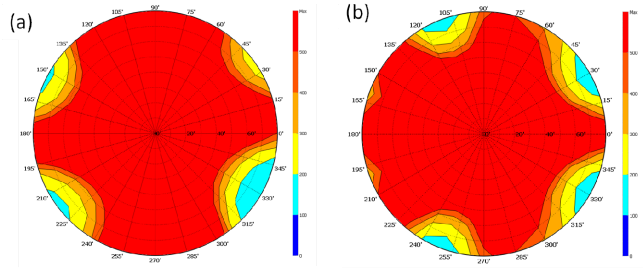

Figure 8. Simulated isocontrast contours for (1) A-FFS, and (b) conventional FFS with a biaxial film. λ=550 nm.

4. Conclusion

The proposed new A-FFS mode can reduce the response time by decreasing the cell gap (4x faster), while keeping transmission >90%. The effect of thickness mismatch on dark state might be a concern, but an acceptable large tolerance range of cell gap is achieved. Also, by choosing a dispersion-matched A-film, good dark state is obtained in the visible range. Similar to FFS, the proposed configuration can also be applied to negative and positive $\Delta\varepsilon$ LC materials.

5. References

[1] S. H. Lee, S. L. Lee, and H. Y. Kim, "Electro-optic characteristics and switching principle of a nematic liquid crystal cell controlled by fringe-field switching," Appl. Phys. Lett. **73**, 2881-2883 (1998).

[2] S. H. Lee, H. Y. Kim, S. M. Lee, S. H. Hong, J. M. Kim, J. W. Koh, J. Y. Lee and H. S. Park, "Ultra-FFS TFT-LCD with super image quality, fast response time, and strong pressure-resistant characteristics," J. Soc. Inf. Disp. **10**, 117-122 (2002).

[3] Z. Ge, S. T. Wu, S. S. Kim, J. W. Park, and S. H. Lee, "Thin cell fringe-field-switching liquid crystal display with a chiral dopant,"Appl. Phys. Lett. **92**, 181109 (2008).

[4] H. Chen, F. Peng, Z. Luo, D. Xu, S.T. Wu, M.C. Li, S.L. Lee, and W.C. Tsai, "High performance liquid crystal displays with a low dielectric constant material," Opt. Mater. Express **4**, 2262-2273 (2014).

[5] W. Maier, A. Saupe, and Z. Naturforsch, Teil A **15**, 287 (1960).

[6] S. T. Wu, "Phase-matched compensation films for liquid crystal displays," Materials Chem. & Phys. **42**, 163-168 (1995).

[7] S. T. Wu, "Birefringence dispersions of liquid crystals," Phys. Rev. A **33**, 1270-1274 (1986).

[8] S. T. Wu and A. M. Lackner, "Mylar-film-compensated π and parallel-aligned liquid crystal cells for direct-view and projection displays," Appl. Phys. Lett. **64**, 2047 (1994).

[9] Y. Chen, F. Peng, T. Yamaguchi, X. Song, and S. T. Wu, "High performance negative dielectric anisotropy liquid crystals for display applications," Crystals **3**, 483-503 (2013).

[10] Y. Chen, Z. Luo, F. Peng, and S. T. Wu, "Fringe-field switching with a negative dielectric anisotropy liquid crystal," J. Display Technol. **9**, 74-77 (2013).

[11] J. W. Ryu, J. Y. Lee, H. Y. Kim, J. W. Park, G.D. Lee, and S. H. Lee, "Effect of magnitude of dielectric anisotropy of a liquid crystal on light efficiency in the fringe-field switching nematic liquid crystal cell," Liq. Cryst. **35**, 407-411 (2008).

[12] H. Zhan, Z. Xu, Y. Wang, Y. Wang, M. Chen, W. Kim, D. Wang, X. Shao, S. Lee, S. Zhao, "Low-voltage, high transmittance fringe-field switching mode liquid crystal for monitor display," Liq. Cryst. **41**, 755-760 (2014).

[13] W. S. Kang, J. W. Moon, G. D. Lee, S. H. Lee, J. H. Lee, B. K. Kim, H. C. Choi, "Retardation free in-plane switching liquid crystal display with high speed and wide-view angle," J. Opt. Soc. Korea. **15**, 161-167 (2011).

[14] E. Jang, S. Jun, H. Jang, J. Lim, B. Kim, Y. Kim, "White-light-emitting diodes with quantum dot color converters for display backlights," Adv. Mater. **22**, 3076-3080 (2010).

[15] Z. Luo, D. Xu, S. T. Wu, "Emerging quantum-dots-enhanced LCDs," J. Display Technol. **10**, 526-539 (2014).